

Directional recrystallization in mechanically alloyed oxide dispersion-strengthened metals by annealing in a moving temperature gradient

W. SHA, H. K. D. H. BHADESHIA

Department of Materials Science and Metallurgy, University of Cambridge/JRDC, Cambridge CB2 3QZ, UK

The directional recrystallization behaviour of mechanically alloyed oxide dispersion-strengthened nickel- and iron-base alloys, MA760 and MA956, has been investigated by annealing in a moving temperature gradient (zone or laser annealing). The directional microstructure produced in MA760 was found to become more isotropic as the zone-annealing speed was increased. At the same time, the recrystallization front tended to become irregular with some nucleation occurring ahead of the main front as the zone-annealing speed exceeded the grain-boundary velocity. These data have been analysed theoretically. Laser-induced recrystallization has also been explored, as another method of annealing a sample in a moving temperature gradient. In the case of the iron-base MA956 alloy, recrystallization occurred directionally along the bar extrusion direction, irrespective of the laser zone-annealing direction.

1. Introduction

Oxide dispersion-strengthened (ODS) materials produced by mechanical alloying (MA) can possess highly anisotropic grain microstructures which are ideal for high-temperature applications [1]. The recrystallization which leads to the development of anisotropic grain structures from deformed or primary recrystallized alloys is known as directional recrystallization. This directional recrystallization can be induced either by zone annealing, which involves the passage of a hot zone along the length of the specimen, or in some cases by isothermal heat treatment of samples in which the grain-boundary velocity is anisotropic.

There are two main classes of mechanically alloyed materials which are of commercial significance, the ODS steels and the ODS nickel-base superalloys, both dispersion-strengthened using Y_2O_3 . All of the as-extruded/hot-rolled nickel or iron base alloys in bar form have an incredibly fine microstructure, consisting of grains which are sub-micrometre in size. The iron alloys exhibit a cold-deformed microstructure in which the ultra-fine grains are elongated along the working direction. Even isothermal heat treatment causes them to recrystallize into coarse columnar grains parallel to the extrusion direction, because the production process causes a pronounced alignment of particles along the extrusion direction.

By contrast with the iron-base alloys, the as-extruded nickel-base superalloys have an ultra-fine equiaxed grain structure which is a product of primary recrystallization, and have a much more uniform distribution of dispersoids [2, 3]. As a consequence,

MA760, when isothermally annealed, recrystallizes into a relatively equiaxed grain structure [3].

The work to be presented here is a part of a wider programme on the process modelling of nickel- and iron-based mechanically alloyed materials. The aim of this programme was to investigate the peculiar recrystallization behaviour of mechanically alloyed metals, in order to enable a better control of their microstructures and mechanical properties. The particular aspect dealt with in this paper is the relationship between the morphology of the recrystallization front and the grain-boundary velocity during recrystallization. It represents a continuation of a previous study on another alloy MA6000 [2], which revealed significant changes in the recrystallization behaviour as the speed of zone annealing was increased.

2. Experimental procedure

The alloys listed in Table I were supplied by INCO Alloys (Hereford, UK) without being given a recrystallization heat treatment. Some of their processing and characterization details can be found elsewhere [3–5]. The essential point is that in this as-received condition, MA956 has a cold-deformed microstructure consisting of sub-micrometre sized elongated grains rich in dislocations [5], whereas MA760 has a sub-micrometre sized equiaxed grain structure in a primary recrystallized state [3].

The general configuration of the radio frequency (r.f.) zone-annealing apparatus have been described in an earlier paper [2]. In the current work, approximately 6.5 mm × 6.5 mm × 25 mm rectangular blanks

were cut from the MA760 alloy, with their major axes parallel or perpendicular to the extrusion direction. The peak temperature during the zone anneal was $1250 \pm 10^\circ\text{C}$. The sample traverse speeds were 0.8 (the lowest speed available), 3.2, 5.6 and 10.0 (the highest speed available) mm min^{-1} . In many experiments, the heating power was deliberately cut off in the middle of the run so that only half of the sample blank was annealed. The measured thermal cycle experienced at a given location as the sample passes through the hot-zone is presented in Fig. 1 as a function of the sample speed.

For laser-induced recrystallization experiments, the samples were approximately $5 \text{ mm} \times 5 \text{ mm} \times 20 \text{ mm}$ rectangular blanks. Laser-beam heating was carried out using a Nd:YAG laser (Lumonics Model JK701), with a focused laser beam size of about 2 mm. The laser power level was set to be approximately 200 W, and the laser traverse speed was 24 mm min^{-1} (the lowest speed available), with a total traverse length of 10 mm for each run. The experiments were conducted in air.

Except where mentioned, all the microscopy was conducted on longitudinal sections. Samples for op-

tical microscopy were etched using a mixture of 2 g CuCl_2 in 20 ml HCl and 60 ml ethanol.

The indentation loads for Vickers hardness and microhardness tests were 196.2 and 0.981 N, respectively.

3. Results and discussion

3.1. Zone annealing parallel to the extrusion direction

Zone annealing of MA760 parallel to the sample extrusion direction gave directional grain growth at all of the travel speeds studied. Fig. 2 shows a series of photomicrographs of the recrystallization front as obtained by stopping the sample heating during its traverse through the hot zone.

The change in grain structure as a function of speed is demonstrated by the data presented in Table II, which also includes the grain aspect ratio of an isothermally recrystallized sample for comparison purposes. The change to the lower grain aspect ratio at the higher speeds is, as discussed in an earlier paper [2], attributed to the fact that the sample moves at a rate which is faster than can be tolerated by all regions of the recrystallization front that develops. Indeed, the hypothesis [2, 6] that recrystallization may nucleate ahead of the main recrystallization front, as the speed is increased is confirmed in Fig. 2d where a few small recrystallization nuclei were recorded in the otherwise unrecrystallized region ahead of the main front. Two other observations support this conclusion: (a) the recrystallization front becomes

TABLE I Chemical composition of mechanically alloyed MA760 and MA956 (wt %)

	Ni	Fe	Cr	Al	Ti	W	Y ₂ O ₃
MA760	Bal.	1.19	19.51	6.00	—	3.41	1.02
MA956	—	Bal.	20.0	4.5	0.6	—	0.5

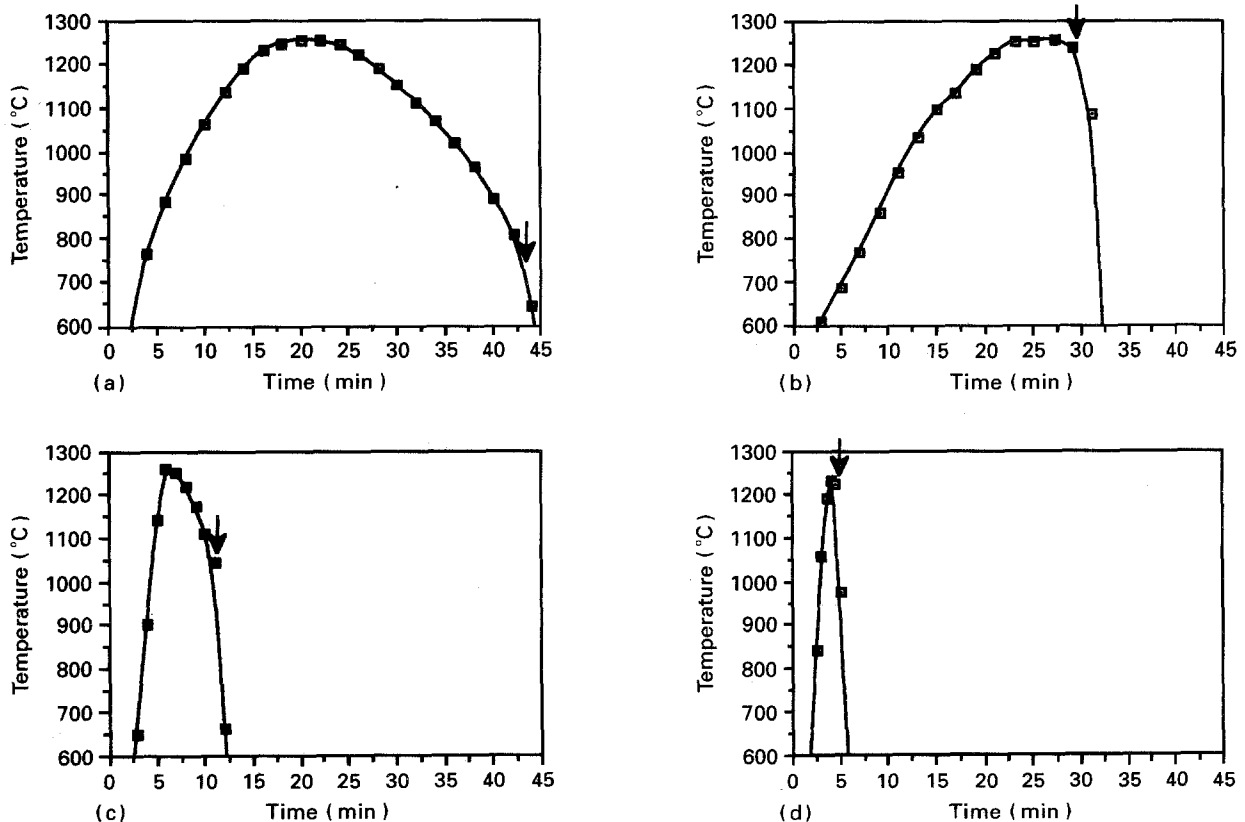


Figure 1 Measured thermal cycles during zone-annealing experiments. Specimen travel speeds are (a), 0.8 mm min^{-1} , (c) 3.2 mm min^{-1} , (d) 5.6 mm min^{-1} . The heating cut-off points are indicated by an arrow in each graph.

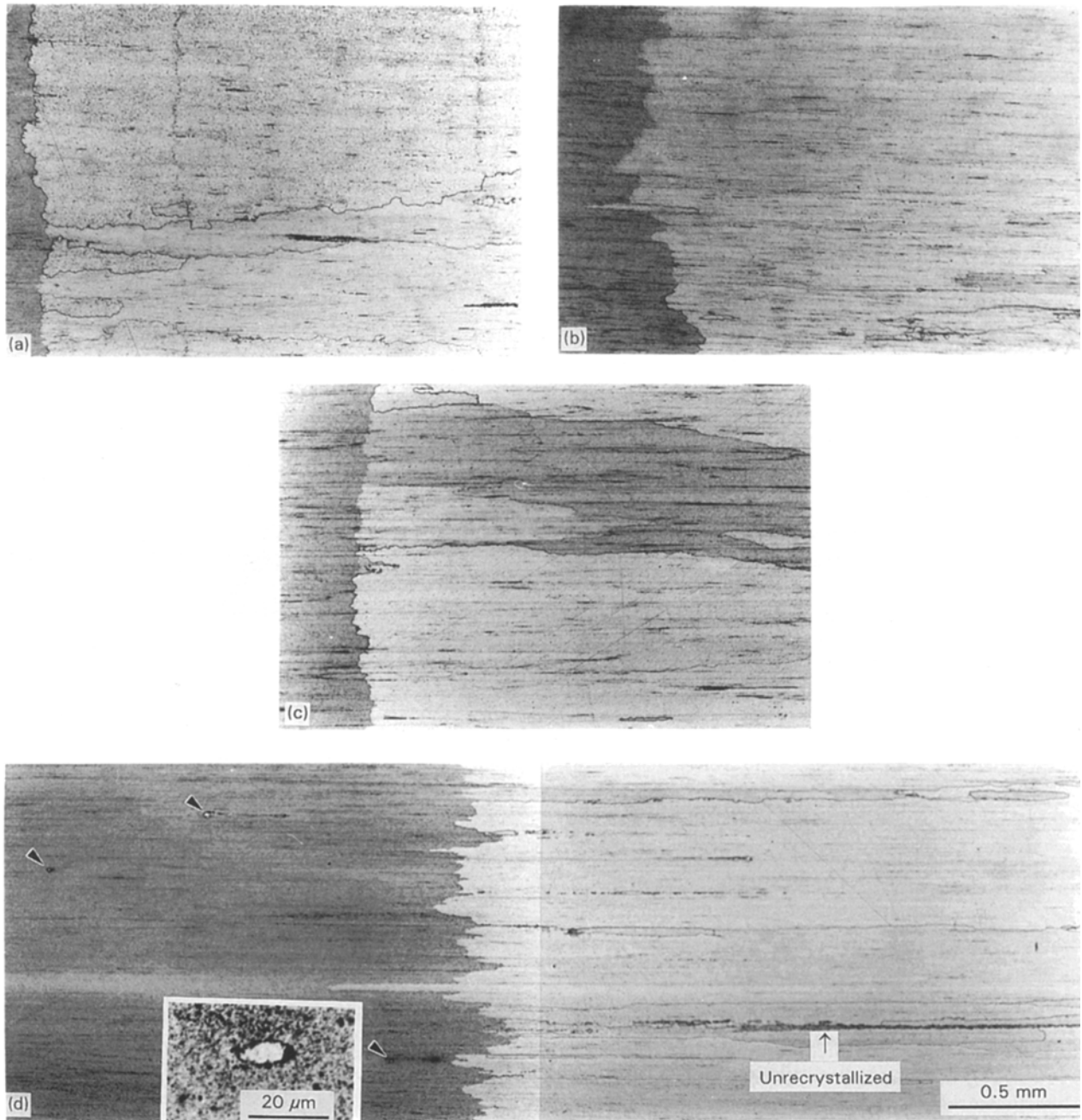


Figure 2 Microstructure of MA760 obtained after zone annealing parallel to the extrusion direction: (a) 0.8 mm min^{-1} ; (b) 3.2 mm min^{-1} ; (c) 5.6 mm min^{-1} ; (d) 10.0 mm min^{-1} . (Nucleation ahead of the main recrystallization front is indicated by arrows in the main micrograph and shown in the inset.) The sample travel direction is from left to right of the micrographs. The darker etching regions are unrecrystallized.

TABLE II Recrystallized grain aspect ratio in samples zone annealed parallel to the extrusion direction

Zone-anneal speed (mm min^{-1})	Approximate grain aspect ratio
0.8	Very large ^a
3.2	26
5.6	9
10.0	8
Isothermal recrystallization	4

^aAlmost all the grains were found to grow through the entire length of the sample.

increasingly irregular as the zoning speed increases; (b) recrystallization becomes incomplete with unrecrystallized regions persisting behind the main recrystallization front, as illustrated for the fastest speed in Fig. 2d. One consequence of the nucleation ahead of

the main front is that the recrystallized region shows a number of finer grains for the highest speed (Fig. 2d).

3.2. Zone annealing normal to the extrusion direction

In most mechanically alloyed bar products, the dispersoids tend to be aligned along the extrusion direction, and this is slightly the case for the MA760 superalloy studied here [3]. As a result, the Zener pinning force is largest for growth normal to the working direction. This is demonstrated by the following “cross-annealing” experiment in which the zone-annealing direction was normal to the extrusion direction (Fig. 3). Clearly, the major growth direction remains along the extrusion direction in spite of the fact that this is normal to the temperature gradient. As in the earlier experiments

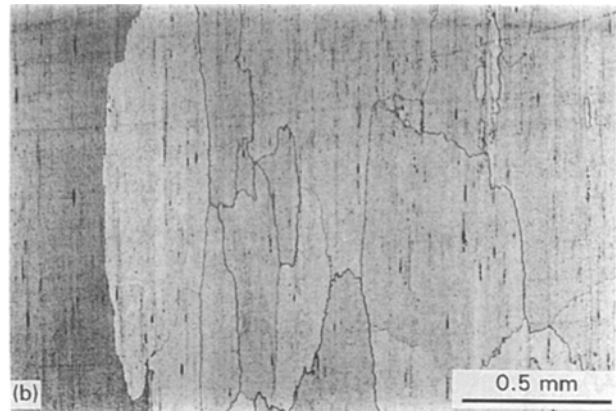


Figure 3 Microstructure of MA760 obtained after zone annealing normal to the extrusion direction (vertical). (a) 0.8 mm min^{-1} ; the sample went through the zone-annealing furnace without interruption. (b) 5.6 mm min^{-1} . The sample travel direction is from left to right of the micrographs. The darker etching region in (b) is unrecrystallized.

(Table II), the grain size along the extrusion direction decreases as the sample speed is increased (Fig. 3).

3.3. Grain-boundary velocity during recrystallization

The grain-boundary velocity, V , during recrystallization is given by [7]

$$V = \delta v \exp(-Q/RT) [1 - \exp(-\Delta G/RT)] \quad (1)$$

where δ and v are the distance and atomic jump frequency across the boundary, respectively, R is the universal gas constant, and Q is an activation energy for the transfer of atoms across the boundary. ΔG is the effective driving force for recrystallization, which does not vary with temperature, but is modified by the particle pinning force (ΔG_p)

$$\Delta G = \Delta G_s - \Delta G_p \quad (2)$$

where ΔG_s is the stored energy in the material. (Other work has shown that ΔG_s in MA760 does not noticeably change when samples are annealed at 1175°C for up to 30 min without recrystallization [8]. Less severe heat treatment will be experienced during the heating part of the zone-annealing cycle. Hence, ΔG is assumed to be independent of the zone annealing speed.)

In the calculation, δ and v were taken as 0.2034 nm ($d_{\{111\}\text{Ni}}$ [9]) and 10^{13} s^{-1} [10], respectively. The activation energy, Q , was taken as that for grain-boundary diffusion, approximated as half of the nickel self-diffusion activation energy [10], i.e. $\frac{1}{2} \times 284518 = 142259 \text{ J mol}^{-1}$ [11]. The stored energy, ΔG_s , measured using differential scanning calorimetry (DSC) was found to be 60 J mol^{-1} for MA760 [3]. Although the particle pinning force, ΔG_p , can be calculated if details of the particle characteristics are known [12, 13], an experimentally determined value was adopted, which was the lowest stored energy recorded capable of inducing recrystallization (20 J mol^{-1}) [8]. The grain-boundary velocity during recrystallization (1250°C) was therefore calculated to be 5.0 mm min^{-1} .

This result agrees well with zone-annealing results (Fig. 2). When the zone annealing speed is higher than the calculated grain-boundary velocity, the recrystal-

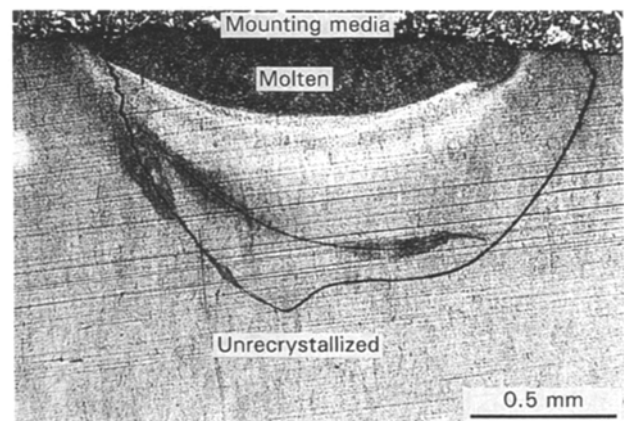


Figure 4 Optical micrographs of the cross-section of a laser-treated MA760 sample.

lization front breaks down with some nuclei appearing ahead of the main front (Fig. 2d).

3.4. Laser recrystallization

In the case of the nickel-base MA760 superalloy, laser heating caused severe cracking (Fig. 4), probably because of the extraordinarily high hardness (HV 762) [3] in the as-received condition. These experiments were therefore abandoned.

Laser annealing of the iron-base MA956 did induce recrystallization in the samples, but only when the samples were severely melted (high heat input). Fig. 5 shows two samples, one with the laser track parallel to the extrusion direction and one normal to it. In both cases, the laser traversed from right to left. There was limited directional recrystallization immediately under the molten zone. In both cases, directional recrystallization only occurred along the extrusion direction, confirming the strong influence of particle alignment in MA956, which has been noted previously [14].

3.5. Hardness measurements

Hardness tests were carried out in the recrystallized regions of zone/cross-annealed MA760 samples. The

results are summarized in Fig. 6. Generally, there is no significant difference amongst the different recrystallized samples, any small variations probably arising from the inhomogeneity of the original material.

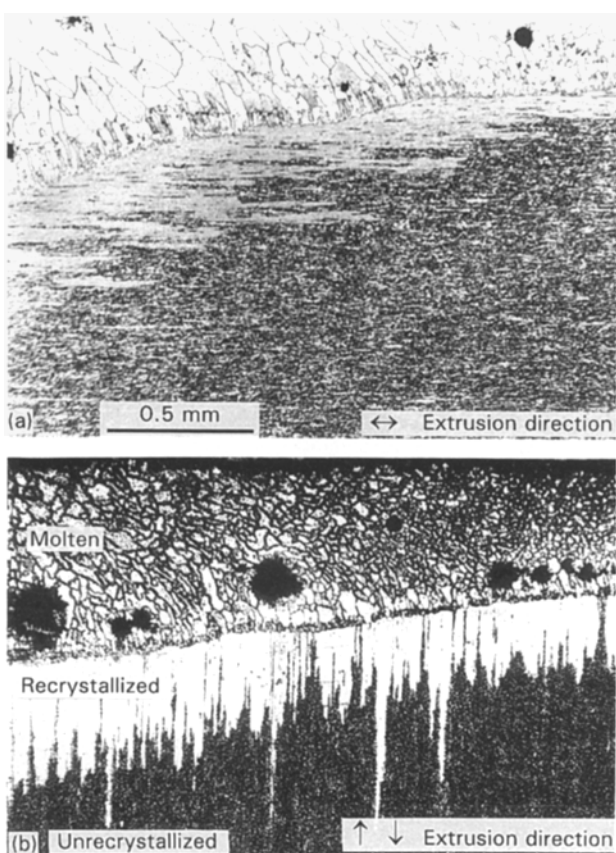


Figure 5 Optical micrographs of laser-treated MA956 samples. Zone annealing is (a) parallel and (b) normal to the extrusion direction of the samples, respectively. The laser travel direction is from right to left of the micrographs.

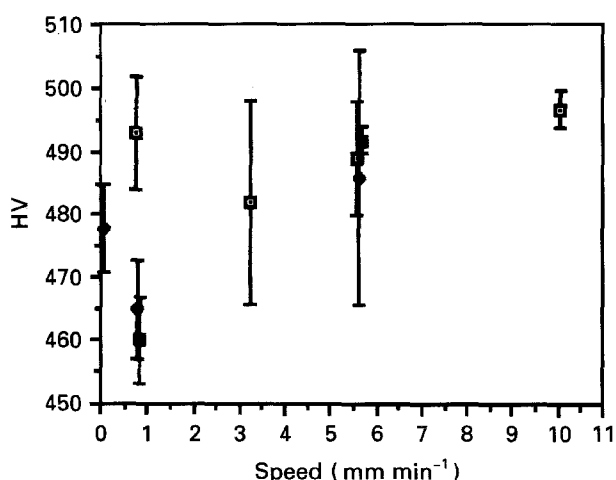


Figure 6 Vickers hardness of (□) zone-annealed (longitudinal section), cross-annealed ((◆) longitudinal and (■) transverse sections), and (◆) isothermally annealed 1250 °C, 1 h, longitudinal section) MA760 samples.

TABLE III Microhardness of zone-annealed (10 mm min⁻¹) MA760 sample

Region	Microhardness
Recrystallized	595 ± 12
Unrecrystallized, ahead of main front	762 ± 14
Unrecrystallized region behind main front	717 ± 33

Microhardness was measured for different regions of a rapidly zone-annealed (10 mm min⁻¹) MA760 sample, to confirm the existence of unrecrystallized areas behind the main recrystallization front (Table III). The microhardness of the unrecrystallized region illustrated in Fig. 2d is slightly lower than that of the normal unrecrystallized region, possibly due to the fact that it is surrounded by recrystallized material together with some recovery.

Finally, the microhardness of different regions in the laser-treated MA956 samples was measured (Table IV). The microhardness of the melted regions is consistently lower than that of the recrystallized regions, indicating the loss of oxide dispersion strengthening.

4. Conclusions

The directional recrystallization behaviour of commercially available oxide dispersion-strengthened alloys, nickel-base MA760, by annealing in a moving temperature gradient, has been investigated. The grain aspect ratio increased with the zone-annealing speed. The recrystallization front becomes increasingly rough, eventually breaking down as the speed of the zone anneal increased beyond that of the calculated grain-boundary velocity. Cross-annealing always resulted in directional recrystallization along the extrusion direction, but the recrystallized grain aspect ratio was reduced when compared with that of isothermally annealed samples.

Laser heating has also been found to induce recrystallization at high heat inputs, but has the disadvantage of causing sample melting. The recrystallization features are otherwise similar to normal directional recrystallization.

Acknowledgements

The authors are grateful to Professor C. J. Humphreys for the provision of laboratory facilities. The research was funded by the Science and Engineering Research Council (UK) under Grant GR/H30427. H. K. D. H. Bhadeshia's contribution to this work was made under the auspices of the "Atomic Arrangements: Design and Control Project", which is a collaborative effort

TABLE IV Microhardness of laser-treated MA956 samples

Laser track direction	Unrecrystallized	Recrystallized	Melted
Parallel to the extrusion direction	348 ± 14	283 ± 9	227 ± 9
Perpendicular to the extrusion direction		298 ± 8	224 ± 20

between the University of Cambridge and Research and Development Corporation of Japan (JRDC). Most helpful were assistance from Dr T. S. Chou, Dr H. Murakami, Mr K. A. Roberts and Dr O. Umezawa, and discussion with Drs I. A. Bucklow, D. J. Gooch and E. R. Wallach. The alloy was kindly supplied by INCO Alloys.

References

1. J. J. DeBARBADILLO and J. J. FISCHER, in "Metals Handbook", 10th Edn, Vol. 2 (American Society for Metals, Materials Park, OH, 1990) p. 943.
2. M. M. BALOCH and H. K. D. H. BHADESHIA, *Mater. Sci. Technol.* **6** (1992) 1236.
3. W. SHA and H. K. D. H. BHADESHIA, *Metall. Mater. Trans.* **25A** (1994) 705.
4. T. S. CHOU, H. K. D. H. BHADESHIA, *Metall. Trans.* **24A** (1993) 773.
5. T. S. CHOU, H. K. D. H. BHADESHIA, G. McCOLVIN and I. C. ELLIOTT, in "Proceedings of the 2nd International Conference on Structural Applications of Mechanical Alloying", Vancouver, British Columbia, September 1993 (ASM International, Materials Park, OH, 1993) p. 77.
6. C. P. JONGENBURGER and R. F. SINGER, in "New Materials by Mechanical Alloying Techniques", edited by E. Arzt and L. Schultz (Deutsche Gesellschaft für Materialkunde, Oberursel, 1989) p. 157.
7. J. W. CHRISTIAN, "The Theory of Transformations in Metals and Alloys: Equilibrium and General Kinetic Theory", 2nd Edn (Pergamon, Oxford, 1975) p. 479.
8. W. SHA and H. K. D. H. BHADESHIA, unpublished research, Cambridge University (1993).
9. "Selected Powder Diffraction Data for Metals and Alloys", 1st Edn, Vol. 1, edited by S. Weissmann, B. Post, M. E. Morse and H. F. McMurdie (JCPDS-International Centre for Diffraction Data, Swarthmore, PA, 1978) p. 91.
10. J. W. CHRISTIAN, "The Theory of Transformations in Metals and Alloys: Equilibrium and General Kinetic Theory", 2nd Edn (Pergamon, Oxford, 1975) pp. 413, 441.
11. D. R. LIDE (ed.) "CRC Handbook of Chemistry and Physics", 57th Edn (CRC Press, Boca Raton, FL, 1993) p. 12-149.
12. K. MURAKAMI, K. MINO, H. HARADA and H. K. D. H. BHADESHIA, *Metall. Trans.* **24A** (1993) 1049.
13. M. J. GORE, M. GRUJICIC, G. B. OLSON and M. COHEN, *Acta Metall.* **37** (1989) 2849.
14. M. M. BALOCH, Ph D thesis, Cambridge University (1989).

*Received 30 June
and accepted 31 October 1994*